



Photocatalytic decontamination of sulfur mustard using titania nanomaterials

P.V.R.K. Ramacharyulu, G.K. Prasad*, K. Ganesan, Beer Singh

Defence Research and Development Establishment, Jhansi Road, Gwalior, India

ARTICLE INFO

Article history:

Received 22 September 2011

Received in revised form

12 November 2011

Accepted 14 November 2011

Available online 22 November 2011

Keywords:

Nanocrystalline titania

Particle size

Sulfur mustard

Decontamination

Photocatalysis

ABSTRACT

Photocatalytic decontamination of sulfur mustard (HD) was studied on titania nanomaterials, and data obtained with irradiation of sunlight and UV-A light was compared with that obtained without irradiation. Role of particle size on photocatalytic decontamination of HD was also investigated. Decontamination efficiency was found to decrease when particle size was increased from 11 nm to 1000 nm. TiO₂ nanoparticles of ~11 nm size of anatase phase exhibited superior decontamination properties relative to larger ones. 100% of HD was decontaminated on their surface within 6 h with irradiation of light. Without irradiation only 24.7% of HD was found to be decontaminated. GC–MS data indicated decontamination of HD to acetaldehyde, carbon dioxide, sulfur mustard sulfoxide, thiodiglycol, acetic acid, etc. due to photocatalysis. Without irradiation only hydrolysis products of HD like thiodiglycol were observed to be formed.

© 2011 Elsevier B.V. All rights reserved.

1. Introduction

Cleansing of surface contaminated with chemical warfare agents (CWA) is the main job we have to do, to make it safe to operate. This can be achieved by application of decontaminants on the surface. Decontaminants remove deadly CWA from contaminated surfaces and render them safe to operate [1–5]. Application of nanosized photocatalysts as decontaminant is interesting as they can be sprayed on contaminated surfaces to assist decontamination by adsorptive removal of CWA. After adsorption, they participate in photocatalytic reactions and assist decontamination of CWA in the presence of light radiation. When a photocatalyst material like TiO₂ is irradiated with light of UV region, whose energy is greater than band gap (3.2 eV), electron–hole pairs are generated [6,7]. These electron–hole pairs finally lead to the formation of hydroxyl radicals and super oxide anion radicals due to their interaction with water molecules or surface hydroxyl groups and oxygen. These species in turn react with CWA and facilitate their decontamination.

On the other hand, physical and chemical properties of TiO₂ materials depend on their particle size. Smaller sized particles are expected to exhibit better chemical reactivity because of their large surface area to volume ratio, increased number of surface defect sites. Particle size also plays crucial role in dynamics of electron/hole recombination process and influences its catalytic

properties. Reduction in particle size also leads to higher photonic efficiency and higher surface charge carrier transfer rate which in turn leads to improved photoactivity of smaller sized particles [8]. In addition to these, TiO₂ is more stable, abundant, non toxic, and economical.

HD is distilled sulfur mustard (bis(2-chloroethyl)sulfide), and a well known CWA. It causes damage to skin, eyes and respiratory system. It alkylates purines in DNA and causes cell damage. These health hazards can be avoided by decontamination of the same [9]. In connection with this, Vorontsov et al. have extensively studied the photocatalytic decontamination of organophosphorous CWA using titania materials both in liquid and gas phases [10,11]. He also studied the photocatalytic decontamination of 2 chloro ethyl ethyl sulfide (CEES), a simulant of HD using titania materials of large size. As per his observations, CEES was converted to its oxidation products [12]. Recently, Prasad et al. have studied sunlight assisted photocatalytic decontamination of HD on ZnO nanoparticles. ZnO nanoparticles decontaminated 100% of HD within 12 h as per the reported data [13]. Although ZnO nanoparticles exhibited promising decontamination properties, they were found to have less stability than TiO₂. ZnO was found to be decomposed to dissolved Zn ions into the reaction media due to photocorrosion [14]. TiO₂ is superior to ZnO and is more stable, abundant, non toxic than ZnO. Inspired by above studies, we have attempted to explore photocatalytic decontamination properties of TiO₂ nanoparticles towards HD in the presence of sunlight or UV-A light. Moreover, sunlight reaching the surface of earth was found to contain 4–5% of UV light which can excite TiO₂ and enable it to destroy CWA [15–17]. For this purpose, we have synthesized TiO₂ photocatalyst

* Corresponding author. Tel.: +91 751 2390169; fax: +91 751 2233482.
E-mail address: gkprasad2001@yahoo.com (G.K. Prasad).

materials of nanosize by sol–gel method and characterized them by XRD, TEM, N₂ BET, and FT-IR techniques. Subsequently, we have studied the effect of particle size of TiO₂ on decontamination of HD in the presence of artificial UV-A light, sunlight, and in the absence of light by using gas chromatography (GC) and gas chromatography mass spectrometry (GC–MS) techniques.

2. Experimental

2.1. Materials

TiO₂ of different sizes: 1000 nm, 200 nm, 70 nm, 35 nm, 16 nm and 11 nm of pure anatase form were used in this study. Of above, TiO₂ having 11 nm, 16 nm and 35 nm sizes were prepared in our laboratory by sol–gel method followed by hydrothermal treatment at 80 °C, 100 °C and 180 °C for 24 h by a reported method [18]. TiO₂ of pure anatase phase having 1000 nm, 200 nm, and 70 nm sizes were purchased from Alfa-Aesar, UK. Titanium tetra isopropoxide (TTIP) was procured from Acros Organics, UK. Dichloromethane, ethanol, ethyl acetate, acetonitrile were obtained from E. Merck India Ltd. HD of 99% purity was obtained from Synthetic Chemistry Division of our establishment (this is a very toxic agent; hence these experiments should be done under the guidance of trained personnel equipped with individual protective equipment only).

2.2. Characterization

Transmission electron microscopy (TEM) measurements were done on Tecnai transmission electron microscope of FEI make. Samples were suspended in 30 mL acetone, and the suspension was sonicated for 30 min. After that, suspension was placed on carbon coated copper grids of 3 mm dia and dried at room temperature prior to the analysis. SEM measurements were done on a FEI instrument. Prepared samples along with commercial ones were characterized by X'Pert Pro Diffractometer (Panalytical, Netherlands) using Cu K α radiation. Nitrogen adsorption measurements were done on ASAP 2020, Micrometrics, USA. GC of Nucon Engineers, India make equipped with FID detector, BP5 (30 m length, 0.5 mm i.d.), OV 17 (1 m length, 3 mm i.d.) columns, and GC equipped with FPD detector and BPX5 column (30 m length, 0.25 mm i.d.) of Thermo Fischer Scientific Corporation, Italy make were used to monitor decontamination kinetics of HD and the formation of reaction products. GC–MS system (5973 turbo) of Agilent, USA make was used for characterization of reaction products. Calibrated equipment manufactured by Technovation India Ltd. was used to monitor carbon dioxide (CO₂) released due to photocatalytic oxidation of HD. FT-IR measurements were done on Perkin Elmer, USA instrument. TiO₂ samples were mixed with dry KBr, ground carefully, made into pellets and were examined from 400 cm⁻¹ to 4000 cm⁻¹.

2.3. Photocatalytic degradation of HD

100 mg of TiO₂ was taken in a quartz tube and 2 μ L of HD was spiked on it. Subsequently, it was irradiated by artificial UV-A light or sunlight. Photo reactor of M/s. Luzchem, Canada make was used for this purpose. UV-A lights of Luzchem, Canada were used for this study. Photocatalysis experiments and reactions in the absence of irradiation were carried out using the setup represented in Fig. 1.

Irradiance of light was measured by digital light meter (SLM 110 model) of A.W. Sperry Instruments, USA with help of adapters provided. Irradiance of UV-A (~360 nm) light was found to be 0.3 mW/cm². A constant airflow of 150 mL/min was passed into the photo reactor from air cylinder of high purity. Gaseous products formed in the reaction were trapped by suction through liquid nitrogen trap @ 40 mL/min, and were analyzed by CO₂ analyzer

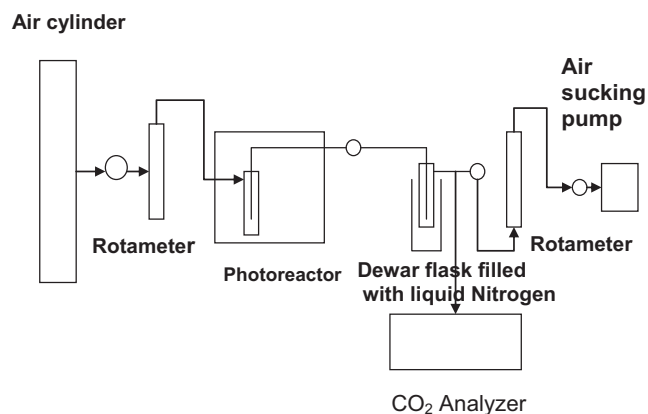


Fig. 1. Schematic diagram of the experimental setup.

and GC. Acetaldehyde was quantitatively measured by calibrating the concentrations using isothermal program at 30 °C. Other reaction products along with HD were monitored by using temperature program from 80 °C to 200 °C at a rate of 10 °C/min after extracting them with acetonitrile. Injection port was kept at 240 °C and detection port (FID and FPD) was kept at 250 °C.

3. Results and discussion

3.1. Characterization of the photocatalysts

TEM was used to determine the crystallite sizes of TiO₂ particles synthesized by sol–gel method followed by hydrothermal treatment. Temperature for hydrothermal treatment was kept at 80 °C, 100 °C, and 180 °C for 24 h. TEM image of TiO₂ particles obtained by hydrothermal treatment at 80 °C shows the crystallites with ~11 nm size (Fig. 2(a)), whereas, image of TiO₂ particles obtained by hydrothermal treatment at 100 °C (Fig. 2(b)) shows the crystallites with size ~16 nm. Crystallite size was found to be increased to ~35 nm when temperature for hydrothermal treatment increased to 180 °C. Particle sizes of purchased samples were found to be 70, 200, and 1000 nm as per the SEM analysis.

According to TEM and SEM images, both synthesized as well as purchased TiO₂ particles were found to have spherical shape. They also show the randomly oriented aggregates of spherical sized nanoparticles whose sizes range from 11 nm to 1000 nm. Enlargement of crystallite size from 11 nm to 35 nm with increased hydrothermal temperature can be ascribed to crystallization of large particles due to increased rate of nucleation and growth at increased temperatures. Moreover, titania crystallites were found to be self assembled in random manner to form aggregates with porous structure. Porous aggregates composed of self-assembled nanoparticles were seemed to be formed due to structural similarity of TiO₂ nanoparticles as well as the charges that were present on their surface. TEM images also show defects, dislocations, and other irregularities at grain boundaries of titania nanocrystallites especially of 11 nm and 16 nm size. These defects were seemed to be formed during the nucleation and growth of nanoparticles.

XRD data of synthesized and purchased titania particles depicted peaks at 2θ values 25.2°, 37.8°, 48.0°, 53.8°, and 62.7°. These peaks can be attributed to the presence of (101), (004), (200), (106), and (215) indices. This XRD pattern (Fig. 3) illustrates 2θ values and relative intensities that match with JCPDS data of anatase phase of TiO₂. The data also illustrated peak broadening in XRD pattern indicating the formation of crystallites with very small size. However, we have not used Scherer analysis of the same to determine particle size as XRD gives ambiguous data of crystallite sizes.

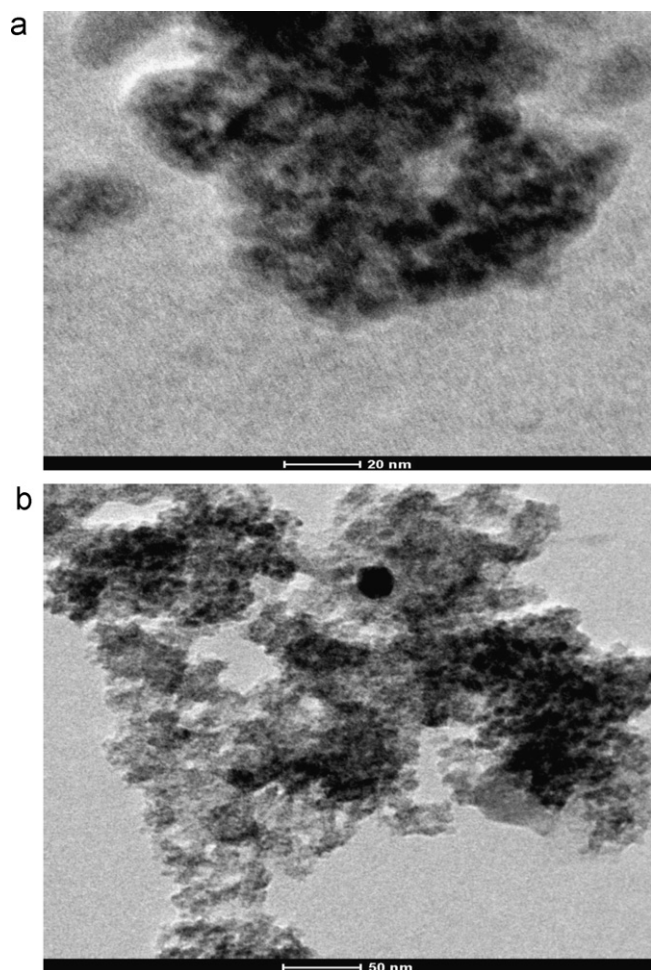


Fig. 2. (a) TEM image of titania material synthesized by hydrothermal method at 80 °C. (b) TEM image of titania material synthesized by hydrothermal method at 100 °C.

Surface area to volume ratio plays a significant role in the catalytic activity of a material along with surface defects present on TiO_2 particles. On decreasing particle size, surface area to volume ratio increases gradually, thereby enhancing the catalytic activity. In addition to the value of surface area, number of surface defects also increases on reduction of size of materials as depicted by

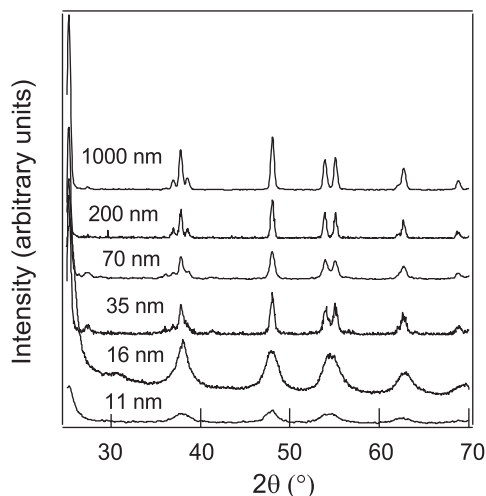


Fig. 3. XRD data of titania materials of various sizes.

Table 1

Nitrogen adsorption data of TiO_2 of various sizes.

Crystallite size (nm)	BET surface area (m^2/g)	Cumulative pore volume (mL/g)	Pore diameter (nm)
1000 nm	16.5	0.03	13.7
200 nm	14.8	0.02	16.8
70 nm	31	0.08	14.8
35 nm	75	0.27	15.4
16 nm	186	0.29	5.0
11 nm	266	0.38	5.3

TEM images. To understand how the values of surface area change, titania particles of various sizes were characterized by nitrogen adsorption measurements. Nitrogen adsorption data indicated type IV isotherm with hysteresis typical of mesoporous materials having pore maxima centred at 5.0 and 5.3 nm in case of particles of sizes 16 nm and 11 nm. The values of surface area and pore volume are given in Table 1. Of all these, titania particles having 16 nm and 11 nm size exhibited high values of surface area 186 m^2/g and 266 m^2/g . All the materials exhibited mesoporosity and values of pore volume were observed to be in the range of 0.09–0.38 mL/g . TiO_2 particles were seemed to aggregate typically to satisfy steric and electrical charge imbalances and formed mesopores. In addition to this, average pore diameter decreased from 13.7 nm to 5.3 nm when size of the material was reduced from 1000 nm to 11 nm. This observation can be ascribed to the fact that, when bigger sized particles aggregated voids of relatively larger size were found to be formed. Whereas on reduction of size, materials with smaller sized voids were found to be formed on aggregation and the same is well illustrated in Table 1.

In addition to surface area to volume ratio, surface hydroxyl groups, surface defects, oxygen vacancies are expected to play major role in providing reactive sites for decontamination of sulfur mustard. They are expected to facilitate hydrolysis and surface complexation reactions of HD in the absence of light, and in the presence of light they were seemed to assist the formation of hydroxyl radicals. Careful examination of FT-IR data indicated the presence of 3204 cm^{-1} , 3281 cm^{-1} , 3335 cm^{-1} , 3391 cm^{-1} , 3426 cm^{-1} , 3463 cm^{-1} , 3563 cm^{-1} and 3488 cm^{-1} frequency bands which indicated the presence of hydroxyl groups with different environments. This data also indicated the presence of OH groups that were attached to both Ti^{3+} and Ti^{4+} ions especially in titania particles of 16 and 11 nm size. This observation further indicated the presence of oxygen vacancies in addition to surface hydroxyl groups. Collectively, surface hydroxyl groups, oxygen vacancies, Lewis acid sites, and other defects play major role in decontamination of HD in the absence of light and in the presence of light to a minor extent.

3.2. Photocatalytic degradation of HD

Only sunlight (250–800 nm) or UV-A light (320–400 nm) irradiation could not decontaminate HD as indicated by blank experiments conducted in the absence of TiO_2 of various sizes. This observation can be attributed to the fact that, photon energy of above mentioned light radiation is not sufficient to excite or decompose HD. However, TiO_2 particles possess some inherent reactivity due to the presence of reactive functional groups. Owing to this, they reacted with HD even in the absence of light and the same is apparent from HD decontamination experiments carried out using TiO_2 particles of sizes 1000, 200, 70, 35, 16 and 11 nm. It can be clearly seen that, on TiO_2 of 1000 nm size only 38.3% of HD was decontaminated in 24 h. Whereas, on TiO_2 of 200 nm size 43.7%, on TiO_2 of 70 nm size 49.0%, on TiO_2 of 35 nm size 57.0%, on TiO_2 of 16 nm size 68.0% and on TiO_2 of 11 nm size 90.0% of HD

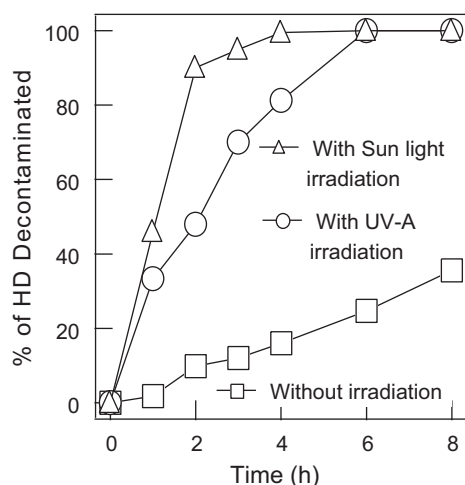


Fig. 4. Decontamination of HD with (sunlight and UV-A light) and without radiation.

was found to get decontaminated without irradiation in 24 h. Data also showed that, percentage of HD decontaminated was found to increase as the crystallite size was decreased from 1000 nm to 11 nm. Decontamination reactions exhibited exponential decrease of HD concentration reflecting pseudo first order behavior. The values of kinetic rate constant and half life were calculated to be 0.023 h^{-1} and 30.1 h for TiO_2 of 1000, 200, and 70 nm sizes and 0.12 h^{-1} and 5.8 h for TiO_2 of 35, 16 and 11 nm sizes. GC–MS data of extracted samples indicated formation of thiodiglycol (m/z values 122, 104, 91, 61, and 43) and hemisulfur mustard (m/z values 140, 141, 111, 109, 104, 73, 63, 45, 27, and 29). Therefore, reactions without irradiation were found to be very slow, contributed only to hydrolysis reactions and surface complexation of HD. They can be attributed to surface hydroxyl groups, Lewis acid sites (Ti^{4+}), defects, oxygen vacancy sites, and moisture present on the titania particles. These observations are consistent with reported data [4].

However, percentage of HD decontaminated was found to be drastically enhanced by photocatalytic treatment in the presence of UV-A or sunlight irradiation. Same is apparent from the data obtained by experiments conducted in the presence of above said light radiations and nano TiO_2 particles of 11 nm size. With irradiation, 100% of HD was found to get decontaminated in 6 h, whereas only 24.7% of HD was found to get decontaminated without irradiation on nano TiO_2 and the same can be seen in Fig. 4.

On the other hand, when compared to TiO_2 particles of larger crystallite size, those having 11 nm size exhibited superior photocatalytic decontamination properties in the presence of sunlight. This observation can be ascribed to high surface area of $266 \text{ m}^2/\text{g}$, more number of oxygen vacancy sites, and other defects. Whereas, on TiO_2 of 1000 nm size only 26.2% of HD was decontaminated in 6 h. Whereas, on TiO_2 of 200 nm size 36.2%, on TiO_2 of 70 nm size 41.3%, on TiO_2 of 35 nm size 90.0%, on TiO_2 of 16 nm size 100% of HD was found to get decontaminated in sunlight in 8 h and on TiO_2 of 11 nm size 100% HD was decontaminated within 6 h. Decontamination efficiency was found to increase as the crystallite size was reduced to 11 nm from 1000 nm.

Acetaldehyde and CO_2 were the gaseous products observed for sunlight assisted decontamination of HD on nano TiO_2 of 11 nm size. Concentration of CO_2 was found to be 100 ppm at 0.5 h. It increased to 340 ppm in 6 h. Acetaldehyde concentration increased from 68.6 ppm to 114.8 ppm in 6 h (Fig. 5).

Whereas, concentration of $(-\text{SC}_2\text{H}_4\text{Cl})_2$ approached a value of 600 ppm in 6 h. It seemed that sunlight facilitated the formation of electrons, holes, and superoxide anion ($\text{O}_2^{\bullet-}$) radicals on the surface on nano TiO_2 which further produced hydroxyl radicals

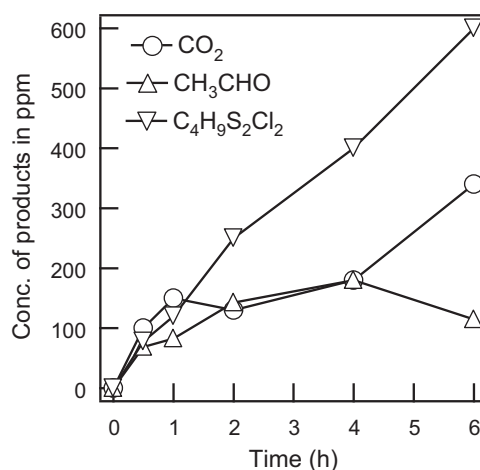


Fig. 5. Product concentration profile of HD decontaminated on nano TiO_2 (11 nm) irradiated with sunlight.

($\bullet\text{OH}$). These reactive species along with other reactive functional groups which are already present on the surface of TiO_2 particle reacted with adsorbed HD molecules and decontaminated it to various reaction products due to photocatalytic degradation reactions, and hydrolysis reactions. In order to investigate the contribution of surface hydroxyl groups and photocatalysis towards HD decontamination in the presence of sunlight the reaction data was analyzed carefully. It indicated that in the absence of light only 24.7% of HD was found to get decontaminated on 11 nm sized TiO_2 particles in 6 h, whereas, in the presence of sunlight 100% of HD was found to get decontaminated in 6 h. This observation clearly indicated that, 75.3% of HD decontamination can be ascribed due to photocatalysis on 11 nm size TiO_2 in the presence of sunlight.

It was also observed that, in the absence of light HD was selectively decontaminated to its hydrolysis products like thiodiglycol. Concentration of thiodiglycol increased from 6.6 ppm to 62 ppm in 8 h on HD exposed nano TiO_2 . In the presence of sunlight, HD was decontaminated to products like CO_2 and acetaldehyde, as mentioned above. In addition, several other products were also detected by GC–MS (Table 2) and the data is consistent with reported data [12]. Hemisulfur mustard and thiodiglycol were seemed to be formed due to hydrolysis of HD and were detected by GC–MS analysis of silylated extract of acetonitrile from TiO_2 surface. In addition to these, 2,2 dichloro diethyl sulfoxide, 2,2 dichloro diethyl sulfone, 1,3-oxathiolane etc., were also detected in acetonitrile extract. 2 chloro ethyl vinyl sulfide, vinyl chloride, acetic acid, 2 chloro ethanol were the minor products observed in acetonitrile extract. These products clearly indicated the occurrence of photocatalytic degradation reactions in addition to hydrolysis.

To understand reactivity of TiO_2 particles and role of their size in decontamination of HD in the presence of UV-A light, experiments were carried out using TiO_2 of variable sizes 1000, 200, 70, 35, 16 and 11 nm. It was observed that, on TiO_2 of 1000 nm size only 73.1% of HD was decontaminated in 24 h. On TiO_2 of 200 nm size 90.4%, on TiO_2 of 70 nm size 92.5%, on TiO_2 of 35 nm size 97.2% was decontaminated in 24 h. On TiO_2 of 16 nm size, 100% of HD was found to get decontaminated within 8 h, and on TiO_2 of 11 nm size 100% of HD was found to get decontaminated in 6 h depicting the photocatalytic decontamination of HD. Percentage of HD decontaminated was found to increase as crystallite size of TiO_2 decreased from 1000 nm to 11 nm. This observation can be attributed to large surface area to volume ratio of particles of smaller size. As the particle size decreased from 1000 nm to 11 nm, the value of surface area increased from $16.5 \text{ m}^2/\text{g}$ to $266 \text{ m}^2/\text{g}$ indicating increased adsorption capacity, increased number defects, surface hydroxyl

Table 2List of products detected due to the photocatalytic decontamination of HD on nano-TiO₂.

Product name	Molecular formula	m/z values
Acetaldehyde	CH ₃ CHO	44, 43, 31, 29, 26, 15
Carbon dioxide	CO ₂	44, 28, 22, 16
2-Chloro ethanol	ClCH ₂ CH ₂ OH	81, 83, 43, 36, 31, 27, 15
Acetic acid	CH ₃ COOH	60, 59, 43, 15
Ethylene oxide	C ₂ H ₄ O	44, 31, 29, 26, 15
2 chloro ethyl vinyl sulfide	C ₄ H ₇ SCI	122, 94, 73, 65, 45, 27
1,3 dithiolane 1 oxide	C ₃ H ₆ OS ₂	122, 110, 106, 98, 73, 66, 46
Ethane thiol	C ₂ H ₆ S	64, 58, 47, 37, 29, 26, 15
1,3 oxathiolane	C ₃ H ₆ OS	106, 78, 73, 64, 53, 45, 27
2,2-Dichloro diethyl sulfone	C ₄ H ₈ O ₂ SCl ₂	127, 92, 63, 27
Bis(2-chloroethyl) disulfide	C ₄ H ₈ S ₂ Cl ₂	190, 155, 128, 92, 79, 63
Hemisulfur mustard	C ₄ H ₉ OSCI	140, 141, 111, 109, 104, 73, 63, 45, 27, 29
Thiodiglycol	C ₄ H ₁₀ O ₂ S	122, 104, 91, 61, 43
2 hydroxy ethyl vinyl sulfide	C ₄ H ₈ OS	104, 91, 61, 43
2,2-Dichloro diethyl sulfoxide	C ₄ H ₈ OSCl ₂	174, 158, 127, 104, 63, 27
Bis(2-chloroethyl thio) methane	C ₅ H ₁₀ S ₂ Cl ₂	204, 158, 127, 92, 63, 27
Vinyl chloride	C ₂ H ₃ Cl	65, 63, 27, 26

groups. Due to increased adsorption capacity more number of HD molecules could have interacted with surface of titania, and reacted with electrons, holes, super oxide anion radicals and hydroxyl radicals that were generated on surface of nanocrystalline titania on irradiation with UV-A light. Collectively, in the presence of UV-A light and nano TiO₂ hydrolysis as well as photocatalytic oxidation reactions contribute to decontamination of HD.

Acetaldehyde and carbon dioxide were the gaseous products formed in large quantities. Concentration of CO₂ increased gradually with time and approached a value of 800 ppm in 6 h and started decreasing and finally reached 700 ppm in 8 h (Fig. 6).

On the other hand, rate of CO₂ generation should be increased because of the gradual increase in amount of acetaldehyde formed. However, acetaldehyde was converted to acetic acid and then to CO₂ and H₂O due to oxidation of carbon atom. Because of this, significant quantity of CO₂ was not observed. Incomplete degradation of surface organic compounds could have also caused low

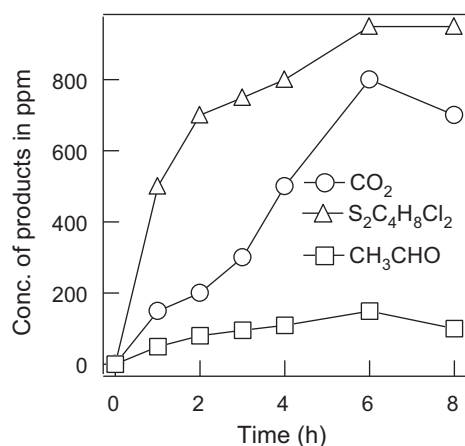


Fig. 6. Product concentration profile of HD decontaminated on nano TiO₂ (11 nm) irradiated with UV-A light.

CO₂ concentration. The concentration of CH₃CHO had reached a maximum value 150 ppm in 6 h and started decreasing indicating catalyst deactivation and surface poisoning due to formation of HCl and H₂SO₄ on the surface. Less volatile products formed on the surface of TiO₂ were studied by extracting with dry acetonitrile. The solution was analyzed by GC-FPD and GC-MS after silylation. Data depicted the formation of bis(2-chloroethyl) disulfide (–SC₂H₄Cl)₂ in major quantity. Concentration of (–SC₂H₄Cl)₂ approached a value of 950 ppm in 8 h of photocatalysis on the surface of titania particle of 11 nm size under UV-A light radiation.

In addition to these, several other products were also detected by GC-MS (Table 2) and the data is similar to that observed in the presence of sunlight [13]. In order to investigate the contribution of surface hydroxyl groups and photocatalysis towards HD decontamination in the presence of UV-A light the reaction data was analyzed carefully. It indicated that in the absence of light only 24.7% of HD was found to get decontaminated on TiO₂ particles of 11 nm size in 6 h as discussed earlier. However, in the presence of UV-A light 100% of HD was found to get decontaminated in 6 h. This observation clearly indicated that, remaining 75.3% of HD decontamination can be ascribed due to photocatalysis on 11 nm size TiO₂ in the presence of UV-A light. In the presence of UV-A light, HD was selectively decontaminated to the products similar to that observed in the presence of sunlight.

3.3. Mechanism of HD photocatalytic degradation

Without irradiation, only hydrolysis and surface complexation reactions seemed to have contributed to decontamination of HD. HD molecules observed to react with TiO₂ in two ways. In one way, they reacted with surface hydroxyl groups that were present on the surface of TiO₂ and formed thiodiglycol, etc. In another way, they reacted with isolated hydroxyl groups (Ti–OH) and Lewis acid (Ti⁴⁺) sites to form surface bound alkoxy species and the same is supported by IR data. These observations are consistent with already reported data [13,4].

IR data indicated disappearance of band at 700 cm^{–1} (C–Cl), change of peak pattern at around 1440 and 1295 cm^{–1} (CH₂–Cl), slight change in peak intensity at ~3352 cm^{–1} (–O–H), and a weak band at ~1100 cm^{–1} (C–O–Ti) further confirming the hydrolysis and surface complexation reactions.

On the other hand, photocatalytic decontamination reaction was stimulated by light radiation. Initially, electrons and holes were seemed to be generated. Holes reacted with water molecules, surface hydroxyl groups and formed hydroxyl radicals (•OH) and protons. Electrons reacted with oxygen molecules and formed superoxide anion (O₂^{•–}) radicals. Hydroxyl radicals, super oxide anion radicals, holes, etc. seemed to have collectively reacted with adsorbed HD molecules and decontaminated it. It seemed that, photocatalytic oxidation of HD started with sulfur radical cations. Firstly the radical cation of HD reacted with superoxide anion or oxygen and formed HD sulfoxide and HD sulfone owing to oxidation of S atom of HD. The radical cation was found to have undergone cleavage of either of C–S bonds, and these alkyl cations reacted with water to produce alcohols and thiols as per the following reactions. This observation was also supported by GC-MS data as it had detected 2 chloro ethanol in acetonitrile extract from titania exposed to light and HD. The other route is the elimination of proton from alkyl radical cation which was assisted by superoxide anion as base to form chloro ethyl vinyl sulfide, hydroxy ethyl vinyl sulfide. The thiyl radicals ClCH₂CH₂S[•] formed due to photo reaction recombined giving the detected products bis(2-chloroethyl) disulfide (–SC₂H₄Cl)₂, bis(2-chloroethyl thio) methane (C₅H₁₀S₂Cl₂). On the other hand, formation of large amounts of acetaldehyde, carbon dioxide and small amounts of acetic acid, vinyl chloride, ethylene oxide, etc., indicated oxidation of C atoms of HD by super oxide

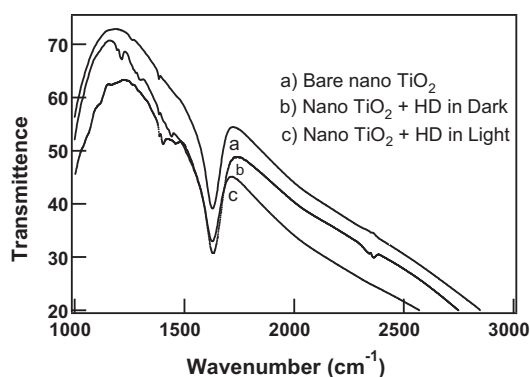


Fig. 7. FT-IR spectra of bare nano TiO₂ (a), nano TiO₂ exposed to HD without irradiation in dark (b), nano TiO₂ exposed to HD with irradiation in light (UV-A light or Sun light) (c).

anion radical. It should also be noted that, mechanism is highly complex and can also follow combinations of mechanisms such as oxidation of C atom, cleavage of C–S bond, oxidation of S atom, hydrolysis of C–Cl bond or elimination of HCl and free radical mechanisms as well. The same is consistent and similar to already reported data [13].

Further, nano TiO₂ was observed to be deactivated after 3rd use due to poisoning of catalysts, i.e., formation of alkoxy species, H₂SO₄ and HCl on the surface of titania. Initially it exhibited 95% of HD decontamination efficiency and the same was maintained when it is re-used after washing with acetonitrile. However, it decreased to 72% after 3rd use and then to 56% after 5th use. Whereas, ~95% HD decontamination efficiency was observed continuously for fifth time when the titania was thoroughly washed with 30% hydrogen peroxide solution followed by washing with copious amounts of water, ethanol and dichloromethane. This can be ascribed to the formation of surface bound alkoxy species as well as sulfonate species and the same is supported by IR data.

Formation of these species was indicated by appearance of a weak band at 1100 cm⁻¹ (–C–O–Ti). An additional band at 1234 cm⁻¹ was also observed further indicating the formation of surface bound sulfate species. However, when washed with hydrogen peroxide surface was cleaned and renewed thus exhibiting better stability and ability to retrieve.

The IR data also showed band at 3240 cm⁻¹ indicating the presence of O–H stretching vibration, a band at a 1630 cm⁻¹ indicating the deformation vibrations of surface hydroxyl groups. Strong band at around 1000 cm⁻¹ depicted the presence of lattice vibrations of TiO₂ in case of IR data recorded for TiO₂ only. In the case of HD adsorbed on TiO₂, a band at 2930 cm⁻¹ indicated C–H vibration of CH₂S, bands at around 1220 cm⁻¹ and 1270 cm⁻¹ correspond to CH₂ vibration of the CH₂–S group which are characteristics of adsorbed HD on nano TiO₂. Band at 700 cm⁻¹ disappeared due to hydrolysis of HD on TiO₂ without irradiation. With irradiation (UV-A or sunlight) the band pattern observed to be changed. Weak bands at 1126 cm⁻¹, 1200 cm⁻¹ illustrated the formation of sulfonate species and band at around 1410 cm⁻¹ indicated the formation of –COOH group typical of acetic acid formed during photocatalytic decontamination of HD on nano TiO₂ (Fig. 7).

Sulfonate species were seemed to strongly bound to the surface thereby deactivating the catalyst, however, on washing with

hydrogen peroxide these species were removed and the surface was rendered clean thereby exhibiting stable photodecontamination activity towards HD. Apparently, it was understood that OH•, O₂•–, electrons, holes have played a collective role in photocatalytic decontamination of HD in the presence of sunlight or UV-A light on TiO₂ particles. Formation of hydroxyl radicals on the surface of TiO₂ nanoparticles in the presence of sunlight or UV-A light was monitored by the reactions with DMSO. Identification of methane sulfonic acid ethyl ester and methane sulfonic acid by GC–MS clearly indicated the formation of hydroxyl radicals (as depicted by *m/z* values at 124, 109, 97, 79, 65, 45 and 96, 79, 65, 48, 31). Hydroxyl radical was found to react with DMSO and converted it to methane sulfonic acid, etc. [19]. When compared to recently reported nano ZnO [13], nano TiO₂ exhibited better decontamination properties. It had decontaminated 100% of HD within 6 h, whereas nano ZnO decontaminated 100% of HD in 12 h thus promising potential use as sorbent decontaminant against CWA.

4. Conclusion

Photocatalytic decontamination of sulfur mustard was studied using titania particles of different sizes and sunlight or UV-A light. With decrease of particle size from 1000 nm to 11 nm, HD decontamination efficiency was found to be increased from 26.2% to 100% within 6 h in the presence of sunlight. Although, HD was found to be completely decontaminated, it was not completely mineralized and it was only partially mineralized to CO₂ under the studied experimental conditions. HD was decontaminated to relatively non toxic products thus promising potential decontamination applications of nano TiO₂. GC–MS data attributed decontamination of HD to oxidation, cleavage of C–S bond, elimination of HCl facilitated by hydroxyl radicals which were formed on the surface of TiO₂ due to photocatalysis.

References

- [1] Y.C. Yang, J.A. Baker, J.R. Ward, Chem. Rev. 92 (1992) 1729–1743.
- [2] B. Singh, G.K. Prasad, K.S. Pandey, R.K. Danikhel, R. Vijayaraghavan, Defence Sci. J. 60 (4) (2010) 428–441.
- [3] G.W. Wagner, L.R. Procell, R.J. O'Connor, M. Shekar, C.L. Carnes, P.N. Kapoor, K.J. Klabunde, J. Am. Chem. Soc. 123 (2001) 1636–1644.
- [4] G.K. Prasad, T.H. Mahato, B. Singh, K. Ganesan, A.R. Srivastava, M.P. Kaushik, R. Vijayaraghavan, AIChE J. 54 (11) (2008) 2957–2963.
- [5] G.K. Prasad, B. Singh, K. Ganesan, A. Batra, T. Kumeria, P.K. Gutcher, R. Vijayaraghavan, J. Hazard. Mater. 167 (1–3) (2009) 1192–1197.
- [6] A. Fujishima, K. Honda, Nature 37–38 (1972) 238.
- [7] A. Fujishima, K. Hashimoto, T. Watanabe, TiO₂ Photocatalysis, Fundamentals and Applications, BKC Press, Tokyo, 1999.
- [8] X. Chen, S.S. Mao, Chem. Rev. 107 (7) (2007) 2891–2959.
- [9] L. Szinicz, Toxicology 214 (2005) 167–181.
- [10] E.A. Kozlova, A.V. Vorontsov, Int. J. Hydrogen Energy 35 (14) (2010) 7337–7343.
- [11] A.V. Vorontsov, E.N. Savinov, C. Lion, P.G. Smirniotis, Appl. Catal. B: Environ. 44 (2003) 25–40.
- [12] A.V. Vorontsov, C. Lion, E.N. Savinov, P.G. Smirniotis, J. Catal. 220 (2) (2003) 414–423.
- [13] G.K. Prasad, P.V.R.K. Ramacharyulu, B. Singh, K. Batra, A.R. Srivastava, K. Ganesan, R. Vijayaraghavan, J. Mol. Catal. A: Chem. 349 (1–2) (2011) 55–62.
- [14] P. Spathis, I. Poullos, Corros. Sci. 37 (5) (1995) 673–680.
- [15] I. Poullos, I. Tsachpinis, J. Chem. Technol. Biotechnol. 74 (1999) 349.
- [16] F. Denny, E. Permana, J. Scott, J. Wang, D.Y.H. Pui, R. Amal, Environ. Sci. Technol. 49 (14) (2010) 5558–5563.
- [17] T.E. Doll, F.H. Frimmel, Catal. Today 101 (3–4) (2005) 195–202.
- [18] Z. Zhang, C.C. Wang, R. Zakaria, J.Y. Wing, J. Phys. Chem. B 102 (52) (1998) 10871–10878.
- [19] P. Popham, A. Novacky, Plant Physiol. 96 (4) (1991) 1157–1160.